Environmental Science & Technology

ARTICLE

pubs.acs.org/est

Diffusion of Nanoparticles in a Biofilm

Thomas-Otavio Peulen[†,‡] and Kevin J. Wilkinson[*,†]

[†]Department of Chemistry, University of Montreal, P.O. Box 6128, succursale Centre-ville, Montreal, Quebec, Canada, H3C 3J7

Supporting Information

ABSTRACT: In order to evaluate the risk of engineered nanomaterials in the natural environment, one must determine their mobility, among other factors. Such determinations are difficult given that natural systems are heterogeneous and biofilms are ubiquitous in soils and waters. The interaction and diffusion of several model nanoparticles (dextrans, fluorescent microspheres, Ag nanoparticles) were studied in situ using confocal microscopy and fluorescence correlation spectroscopy in a biofilm composed of *Pseudomonas fluorescens*. For the most part, relative self-diffusion coefficients decreased exponentially with the square of the radius of the nanoparticle. The precise growth conditions of the biofilm resulted in a variable density of both exopolymers and microbes, which was also shown to be an important parameter controlling the diffusion of the nanoparticles. Finally, the charge of the nanoparticles appeared to be important; for a dense bacterial biofilm, a greater than predicted decrease in the self-diffusion coefficient was observed for the negatively charged nano Ag.

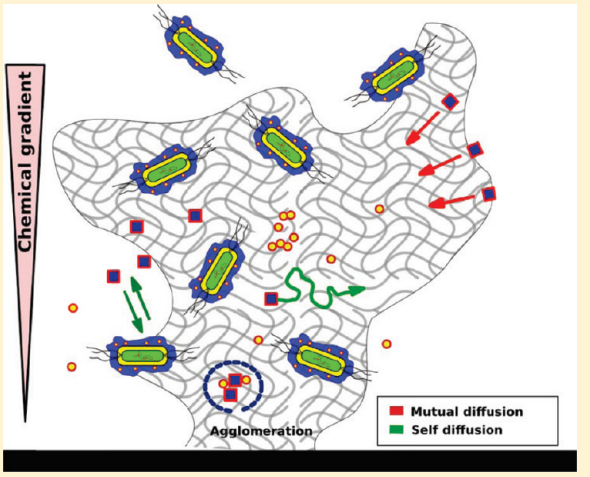

INTRODUCTION

While most evaluations of environmental risk are performed on planktonic organisms, the vast majority of microorganisms live and grow in highly structured aggregates such as biofilms and flocs.[1] Biofilms and flocs are composed primarily of microbial cells and extracellular polysaccharides and proteins (extracellular polymeric substances or EPS[2]). They are highly structured but heterogeneous microenvironments, featuring chemical gradients of important parameters such as oxygen, pH, and nutrients.[3] In soils, the transport of colloids and nanoparticles will be modified by interactions with biofilms and changes to the hydrodynamics of the soil due to the presence of biofilm.[4] Furthermore, microorganisms in a biofilm can facilitate the degradation, sorption, or generation of colloids and nanoparticles.[5] Nonetheless, since the dominant transport mechanism in biofilms and flocs is diffusion,[6] the mobility and bioavailability of nanoparticles will largely depend upon their diffusion coefficients, which will be related to their size and physicochemical characteristics, as well as the nature of the biofilm. Although the diffusion of solutes has been studied for several biofilms, there is still little consensus on effective diffusion coefficients, with reported values typically varying over several orders of magnitude for even well studied probes (e.g., fluorescein[7−9]).

Diffusion coefficients in gels and biofilms can be determined either by measuring mass transport due to differences in chemical potential (mutual diffusion coefficients: Fourier transform infrared;[10] half-cell studies[11]) or by measuring solute self-diffusion (fluorescence correlation spectroscopy (FCS);[12−15] fluorescence recovery after photobleaching (FRAP);[11] pulse field gradient nuclear magnetic resonance[16]). In fluorescence correlation spectroscopy (FCS), fluorescence fluctuations originating from the diffusion of a substrate through a small, confocally defined optical volume (ca. 10^{-15} L) are quantified using an avalanche photodiode detector.[17] FCS provides dynamic information about a wide range of molecular processes in the nanoseconds to milliseconds range.[18−20] Since FCS diffusion coefficients are determined from the Brownian motion of the fluorophore, they are self-diffusion coefficients, which are not affected by the binding of fluorophore to the biofilm or by a decrease in chemical flux. FCS has the additional advantage of being able to determine diffusion coefficients on a submicrometer distance scale,[21] which when repeated (mapping) provides an indication of biofilm heterogeneity.[11,15] In contrast to FRAP, fluorophore concentrations and laser intensities are smaller in FCS, reducing errors caused by biofilm perturbation or a local warming.[22] Until recently, only a few FCS measurements, covering only a small range of solute sizes, have been performed in biofilms.[12−15]

Hydrogels have often been proposed as a simple model for understanding diffusion in a constrained medium such as a biofilm.[8,11] The diffusivity of a solute through a physically cross-linked hydrogel decreases with increased gel cross-linking, increased solute size, or decreased gel porosity.[23,24] Indeed, one

Received: October 12, 2010
Accepted: March 9, 2011
Revised: March 7, 2011
Published: March 24, 2011

simplified model (see also Supporting Information) relates decreases in the relative diffusion coefficient of a solute with the square of the solute cross-section.

$$D_g/D = B \cdot \exp(-A \cdot R_h^2) \quad (1)$$

where D_g (or D_{bio}) is the diffusion coefficient in the gel (or biofilm), D_0 is the diffusion coefficient in water, R_h is the hydrodynamic radius of the solute, B is the probability of finding a hole unhindered by polymer (dependent on the solute's cross-sectional area or volume), and A is a structural constant related to the heterogeneity of the gel network.[25] Given that it only takes solute and not biofilm characteristics into account, this simple model is clearly an oversimplification. Nonetheless, it is a useful test of whether or not the substrate follows classical diffusive behavior or whether more complex models (e.g., those taking into account anomalous diffusion) need to be employed.

The aim of the present study was to quantify the diffusion of several model nanoparticles (dextrans: Dx; carboxylated microspheres: MS; Ag nanoparticles: nAg) in an environmentally relevant biofilm of *Pseudomonas fluorescens*.[26] Diffusion coefficients were determined using FCS for nanoparticle standards of known sizes in order to first test the predictions of the classical diffusion model (eq 1). Given that the structure and composition of the biofilm can influence diffusion, two biofilms, of different compositions, were characterized.

MATERIALS AND METHODS

Particle Labeling. The carboxylated nAg were obtained from Vive Nano (Product Number: 13010 L). They were covalently labeled with Nile Blue A (**NBA**) and/or Rhodamine 123 (**Rh123**) using conventional 1-ethyl-3-(3-dimethylamino propyl)-carbodiimide/*n*-hydroxysuccinimide coupling chemistry[27] (Supporting Information). The labeling was performed under mild reaction conditions, using low fluorophore concentrations (ca. 1.5 fluorophores per nAg) to ensure that it was minimally perturbing. After labeling, the particles were extensively dialyzed (24 h) against a 9:1 water/ethanol mixture in order to remove surplus reactants. Measurements of electrophoretic mobilities (ZetaSizer Nano Zen4003) and transmission electron microscopy (TEM) were performed before and after particle labeling.

Nanoparticle Sizes. FCS was used to determine the sizes of the nanoparticles in water, prior to their addition to the biofilm.[28,29] Diffusion coefficients of the labeled dextrans, carboxylated microspheres, and nAg were transformed to hydrodynamic diameters using the Stokes−Einstein equation. Sizes of nAg were also evaluated by TEM (JEOL JEM 2100F). In that case, a droplet containing 5 mg L^{-1} of nAg was pipetted onto a 400 mesh, carbon coated Cu TEM grid and air-dried.[28] For each experimental condition, over a hundred particles were imaged and measured; particle diameter distributions were determined with SigmaSCAN (Systat software inc.).

Biofilm Growth. Overnight cultures of *P. fluorescens* (strain ATCC 13525) were prepared by transferring frozen stock cultures into a nutrient broth medium consisting of 5 g L^{-1} peptone and 3 g L^{-1} meat extract. After 12 h, 10 mL of autoclaved growth medium, consisting of 1.5 g L^{-1} glucose, 0.2 g L^{-1} $(NH_4)_2SO_4$, 1.5 g L^{-1} Na_2HPO_4, 750 mg L^{-1} KH_2PO_4, 1.3 g L^{-1} NaCl, 95 mg L^{-1} $MgCl_2$, 44 mg L^{-1} $CaCl_2$, 0.6 mg L^{-1} thiamine, and either 0.1 mM or 0.01 mM $FeCl_3$,[2] was inoculated with 40 μL of the overnight culture. Biofilms were incubated for 9−12 h at 26 °C in the 0.5 mL wells of the chambered borosilicate cover glasses (Lab-Tek 155411).

Diffusion Measurements in the Biofilms. FCS measurements were performed on a Leica TCS SP5 laser scanning microscope using a laser excitation at 488 nm, 514 nm (Ar ion), or 561 nm (DPSS Nd:YVO_4) under diffraction limited conditions. Fluorescence intensity fluctuations were followed in the emission ranges of 500−530 nm and/or 607−683 nm. Diffusion coefficients were determined for fluorescent dyes (Oregon Green, **OG**, Invitrogen; Rhodamine 6G, **Rh6G**, Invitrogen; Rhodamine 110, **Rh110**, Invitrogen; **Rh123**, Invitrogen; Rhodamine B, **RhB**, Sigma Aldrich; Nile-Blue A, **NBA**, Sigma Aldrich), commercially labeled neutral dextrans (Dextran 3k labeled with Texas Red, **Dx3k**; Dextran 10k, 40k, and 70k labeled with tetramethyl rhodamine, **Dx10k**, **Dx40k**, **Dx70k**; Invitrogen), dyed microspheres (**MS**, carboxylated polymer microspheres labeled with Dragon Green; sizes: 57, 92, 135 nm; Bang Laboratories), and the labeled nAg.

Just before starting an experiment, the growth medium overlying the biofilms was carefully removed and replaced by a small quantity of 1 mM HEPES (pH 7.2) containing the fluorescent probes. Biofilms were equilibrated for 20 min, and all FCS measurements were performed within 1.5 h. Diffusion coefficients were also determined in 1 mM HEPES under otherwise identical conditions. Representative diffusion coefficients were obtained by measuring the diffusion of the probes at a minimum of 9 different positions in the microcolonies. In order to minimize the effect of any macroscopic movement of the microcolonies and to ensure reproducibility, all measurements were performed on an active dampening, antivibration table (Table Stable ltd.) with the laser focused in mechanically stable regions of the biofilm, i.e., no more than 40 μm from the coverslide surface. Optical errors were reduced by performing reference measurements using the same multiwell cover glass as the sample (constant slide thickness) and by always measuring at defined distances from the slide (constant beam astigmatism).[21]

Data acquisition times were minimized (Table S4, Supporting Information) by choosing carefully optimized excitation conditions (fluorophore concentrations, laser power, laser wavelength near excitation maxima). Absolute values of the diffusion coefficients were obtained by first calibrating the system in water using compounds with known diffusion coefficients: 9.7 nM Rhodamine 6G (**Rh6G**); 2.5 and 10 nM **Rh123**; 10 nM Oregon green (**OG488**); and 2.5 nM **Rh110**.[30,31] In all measurements, the confocal shape parameter ω_{xy} was close to its optimal value as determined by the system optics and laser wavelength (see Supporting Information). Autocorrelation decays were fitted to the above-described model using the Levenberg−Marquardt algorithm implemented in the ISS software (version 3.7) with either a one or two component model for particle diffusion assuming a 3D-Gaussian beam profile with an additional bunching term to account for triplet states (Supporting Information). In some cases, an anomalous diffusion model with an additional fitting parameter α was necessary to best fit the data (numerical values for α are given in Supporting Information).

RESULTS AND DISCUSSION

Determination of Particle Sizes. Particle diameters were determined from diffusion coefficients obtained by FCS. For the dextrans, diffusion coefficients decreased with increasing molar mass, in line with recent literature values.[15,32] On the

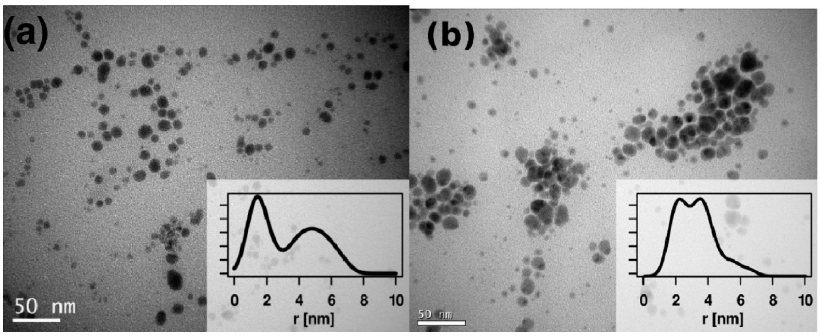

Figure 1. TEM images and size distributions of the silver nanoparticles collected from a 5 mg/L solution of nAg following drop deposition on a 400 mesh Cu, C-coated grid. (a) Unlabeled nAg, polydispersity index (PDI) = 1.4 (number of particles = 383, shape factor = 0.77). (b) nAg labeled with both rhodamine 123 and Nile Blue A, following dialysis. PDI = 1.2 (number of particles = 158, shape factor = 0.73).

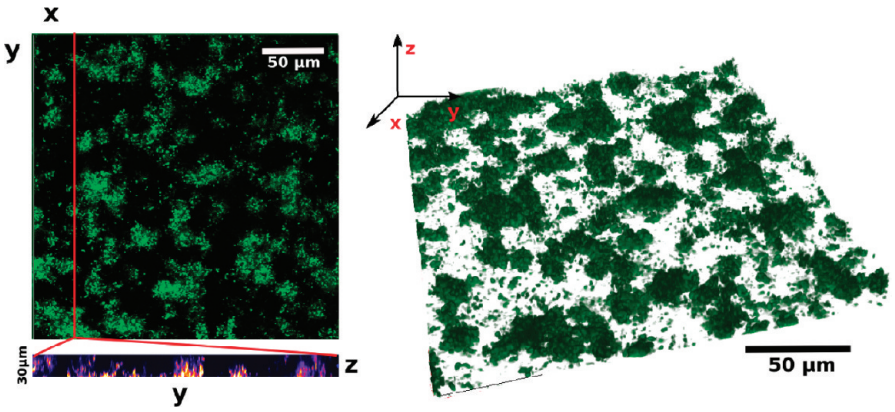

Figure 2. Confocal laser scanning microscopy (CLSM) image of biofilms grown in the presence of 0.01 mM Fe(III); the images were acquired using the reflection mode of the microscope. Due to the lower reflectivity of the microcolonies grown in media containing 0.1 mM Fe, no 3D-reconstruction of that biofilm is presented.

basis of calculations using the Stokes−Einstein equation, under the assumption that the nanoparticles were compact spheres, hydrodynamic radii of 0.9 to 3.2 nm were calculated, also similar to literature values.[33] For the carboxylated microsphere standards, measured hydrodynamic diameters were very close to those provided by the manufacturer: 49.6 ± 4.2 nm for the 57 nm standard, 96 ± 3.8 nm for the 92 nm standard, and 135 ± 8.4 nm for the 135 nm standard. FCS and TEM results confirmed that the stabilized nAg were largely unaggregated in water. Average hydrodynamic diameters of 2 ± 0.4 nm were obtained by FCS in good agreement with the size range provided in the manufacturer's product specification sheets (i.e., 90% in the range of 1−10 nm as determined by TEM; Vive Nano). Although a few particles with diameters up to 50 nm were observed by TEM, size distributions showed that majority of the nAg particles ranged between 2 and 10 nm (Figure 1).

Biofilm Characterization. No two biofilms are identical. In order to evaluate the relative importance of the biofilm characteristics on the diffusion of the nanoparticles, biofilms were grown under two conditions known to strongly influence the growth and morphological properties of the biofilms, as determined by confocal laser scanning microscopy and crystal violet staining.[34] For biofilms grown in 0.01 mM Fe(III), a prolonged lag-phase was observed for the bacteria as compared to those grown in 0.1 mM Fe(III). Furthermore, at the lower Fe concentration, biofilms were more dense and compact, with mushroom like microcolonies that strongly adhered to the glass surfaces (Figure 2). In contrast, in the growth medium containing 0.1 mM Fe(III), bacteria appeared to overproduce EPS and were much more sparsely distributed, in patchy microcolonies and flocs that adsorbed poorly to the glass surfaces of the cover slide. Somewhat counterintuitively, microcolonies grown at the lower Fe(III) concentration had considerably higher cell densities than those grown at the higher concentration. Similar results were found for independent experiments performed in flow cells (data not shown).

Diffusion of the Model Nanoparticles in the Biofilms. Even though the diffusion of solutes is a critical aspect to quanti fying contaminant chemodynamics,[35] there are few data and little consensus for diffusion coefficients in environmental biofilms.[7−9] To some extent, the observed variability in the literature is caused by differences in experimental protocols or the nature of the measurement technique. Indeed, FCS does not measure the diffusive flux of fluorescent substrates resulting from concentration gradients (i.e., mutual diffusion coefficients) but rather the local (self) diffusion coefficient in a ca. 1 μm^3 confocal volume. In order to ensure that the results were representative of the biofilm as a whole, 30−150 independent measurements were made at several different zones of the biofilm (Table 1). In addition, diffusion was quantified for biofilms cultivated in both 0.01 and 0.1 mM Fe(III).

Background fluorescence was initially a concern given that *P. fluorescens* produces water-soluble fluorescent pigments called pyoverdines.[36] Fortunately, the fluorescence of the pyoverdines could be bleached prior to data acquisition of the fluorescent

Table 1. Summary of the diffusion coefficients of the nanoparticles and solutes measured by FCS.[a]

		D_{H2O} [$\mu m^2/s$]		R_h [nm]		D_{bio}/D_{H2O} [b]				
colony type	sample	mean	SD	mean	SD	mean	SD	n	m	charge
0.01 mM Fe	Rh110	430	30	0.5	0.0	0.70	0.16	15	3	negative
	Rh123	440	30	0.5	0.0	0.85	0.19	14	3	positive
	Dx 3000	241	17	0.9	0.1	0.83	0.16	313	9	neutral
	Dx 10000	166	34	1.3	0.3	0.62	0.11	279	13	
	Dx 40000	79	13	2.8	0.4	0.46	0.10	212	11	
	Dx 70000	67	6	3.3	0.3	0.27	0.05	269	15	
	nAg	211.8	44.0	1.03	1	0.13	0.11	30	3	negative
0.1 mM Fe	Rh6G	400	30	0.5	0.0	0.77	0.10	72	9	positive
	RhB	420	30	0.5	0.0	0.80	0.18	72	9	neutral
	Dx 3000	241	17	0.9	0.1	0.81	0.15	189	7	
	Dx 10000	166	34	1.3	0.3	0.68	0.12	72	9	
	Dx 40000	79	13	2.8	0.4	0.79	0.17	99	3	
	Dx 70000	67	6	3.3	0.3	0.66	0.12	126	5	
	MS57	8.80	0.74	24.8	2.1	0.61	0.16	108	4	negative
	MS92	4.55	0.18	48.0	1.9	0.66	0.15	68	4	
	MS135	3.23	0.11	67.5	2.2	0.59	0.11	51	3	
	nAg	211.8	44.0	1.03	1	0.86	0.37	51	3	

[a] Diffusion coefficients measured in water (D_{H2O}) and relative diffusion coefficients D_{bio}/D_{H2O} (D in biofilms with respect to water) are presented. Probe abbreviations: Rhodamine 110 (Rh110), Rhodamine 123 (Rh123), Dextran (Dx), Rhodamine B (RhB), carboxylated microspheres (MS). R_h is the hydrodynamic radius that is estimated using the Stokes Einstein equation; n: number of measurements; m: number of microcolonies where measurements were performed; SD: the standard deviation. [b] D_{bio}/D_{H2O} was determined (see Supporting Information) by fitting histograms of the relative diffusion time distribution; the mean and SD are given by the position and width of the distribution (also see Supporting Information).

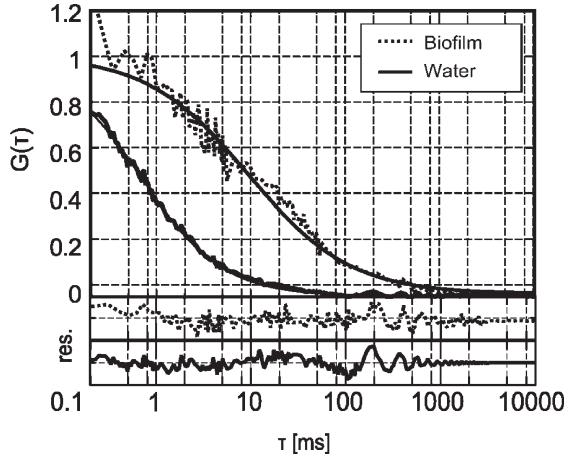

Figure 3. Typical autocorrelation decays for the nAg measured in water and in the bacterial (*P. fluorescens*) cell clusters ([Fe] = 0.01 mM). Solid black lines are fitted to the accumulated data (dashed = biofilm, solid = water). Residuals (res.) are presented on the lower portion of the figure. The fluctuation in the residuals at longer correlation times are mainly caused by intensity fluctuations of the solid state laser used here (561 nm DPSS Nd:YVO_4).

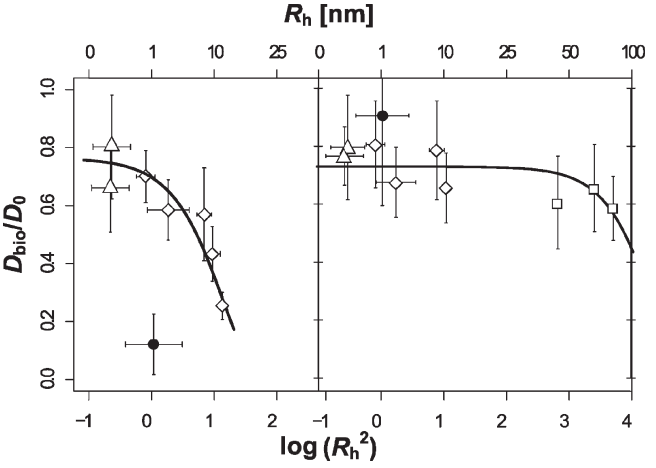

Figure 4. Relative diffusion coefficients in the bacterial microcolonies as a function of solute size for colonies grown in media containing 0.01 mM Fe (left) and 0.1 mM Fe (right). Data points correspond to averages obtained for Rh110 and Rh123 (left) or RhB (right): Δ; labeled dextrans (3k, 10k, 40k, 70k): ◊; dyed carboxylated polymer nanospheres (57 nm, 92 nm, 135 nm): □; and nAg: ●. In the dense bacterial cell clusters (0.01 mM Fe, left), no diffusion of the dyed nanospheres was measurable. The solid line corresponds to a fit that was obtained from eq 1 (excluding the nAg data points) using the following parameters for the curve fitting: left, $A = 0.09\ nm^{-2}$, $B = 0.85$; right, $A = 50\ \mu m^{-2}$, $B = 0.73$.

probes, resulting in the observation of stable autocorrelation decays in the biofilms, albeit with higher baseline noise (Figure 3). Furthermore, the constant offset of the autocorrelation function (ACF) could be easily corrected when fitting the autocorrelation decay. Finally, **NBA** was excited using a laser line (561 nm) that was substantially higher than for the pyroverdines (λ^{ex}_{max} = 460 nm), which allowed us to distinguish spectroscopically between the two fluorophores.

Diffusion coefficients measured in the biofilms were consistently smaller than those determined in water (i.e., $D_{bio}/D_0 < 1$; Figure 4). For the smallest solutes and nanoparticles (<5 nm), diffusion coefficients were 60−80% of those found in water, irrespective of the Fe concentration. The observation of a fairly

constant, ca. 30%, reduction of D for the smaller substrates is indicative of an increased tortuousity (path length) of the solutes and/or an increased viscosity of the biofilm.

For much larger nanoparticles (57, 92, 135 nm) in the dense (low Fe) biofilms, little penetration of the biofilms was observed; diffusion was effectively negligible, and no diffusion coefficient could be determined. Indeed, diffusion of the larger nanospheres was only measurable in microcolonies that were formed under high Fe conditions (loose flocs). In the intermediate size range (1−100 nm), diffusion coefficients decreased rapidly with probe size for both microcolony types (Table 1). Indeed, relative diffusion coefficients (D_{bio}/D_0) decreased exponentially with the square of the solute radius, in line with observations made previously in hydrogels[25] and in biofilms of *Pseudomonas putida*[11] and *Lactococcus lactis*[12,13] (eq 1). While the steep decrease of D_{bio}/D_0 was observed for the intermediate sized nanoparticles (>57 nm) in the loose microcolonies, in the dense bacterial microcolonies, relative diffusion coefficients decreased significantly for the two largest dextrans (M_w of 40 000 and 70 000), corresponding to nanoparticle sizes (diameters) of 3.6 and 4.9 nm. These results suggested that the effective poresize of the biofilm was in the range of 50 nm for the loose flocs but decreased below 10 nm for the dense biofilms. Clearly, nanoparticle (1−100 nm) mobilities in the environment are likely to be significantly hindered by the presence of biofilms.

Even though eq 1 only takes the increased viscosity and tortuosity of the biofilm into account, it describes nearly all experimental data, within experimental error (p-value ≤0.1 in a two sided F-test). The success of this equation, for both of the biofilms and for most of the model nanoparticles (dextrans, microspheres) suggests that these are the two most important effects controlling diffusion in these biofilms. Neither particle aggregation within the biofilms nor the coupled diffusion of the nanoparticles with biofilm components needed to be invoked to explain the vast majority of results in Figure 4.

The shape of the autocorrelation curves in the biofilm changed somewhat with respect to those obtained in solution, in particular, for solutes with the smallest diffusion coefficients and for the densest microcolonies (Figure 3). In solution, the autocorrelation decay could be easily characterized by a single characteristic diffusion time, τ_D, whereas in the biofilms, the tailing of the autocorrelation decay at higher correlation times suggested that the solutes were either adsorbed by the biofilm matrix or entrapped by the bacterial cells. A similar effect, observed previously for measurements of dextrans in hydrogels, was attributed to the anomalous diffusion of the solutes caused by molecular crowding and the presence of obstacles to diffusion.[37,38] Anomalous diffusion can be quantified by the value of α that is determined from the autocorrelation function. Values were in the range of 0.89−1.01 (Table S2, Supporting Information), effectively indicating some nonelastic interactions of the biofilm matrix and the nanoparticles.

Diffusion and Adsorption of the nAg in the Biofilms. In the loose flocs that formed at low Fe, the diffusion coefficient of nAg decreased only slightly, to 86% of the value in water, well within the range that was expected on the basis of size alone (Figure 4). In contrast, for the dense microcolonies formed at high Fe, a much smaller diffusion coefficient than predicted was observed, corresponding to a D_{bio}/D_0 value of 0.13 (Figure 4, Table 1). As above, measurements were repeated numerous times in different zones of the biofilm to ensure reproducibility. While a statistically valid number of measurements were performed for the nAg, it must be noted that a large number of attempts to determine D_b were also unsuccessful. We hypothesized that a large proportion of the fluorescence was immobile due to the accumulation of nAg in distinct zones of the microcolonies. In FCS, sorbed fluorophores increase background noise, making it more difficult to quantify the fluorescence intensity fluctuations that are used to determine diffusion times. In order to confirm that hypothesis, laser scanning microscopy was performed (λ_{ex} = 633 nm; λ_{em} = 650−690 nm) following a 4 h equilibration of the two biofilms with 20 mg L^{-1} NBA labeled nAg. Significant nAg fluorescence was observed (Figure 5, middle), for the most part, closely associated with the bacterial cells of the biofilm (Figure 5, right). In addition, the nAg appeared to accumulate to a much greater extent in the dense biofilms as compared to the loose flocs. The EPS in the biofilms are globally, negatively charged and known to associate metal cations and some macromolecules including proteins, DNA, lipids, and even humic substances.[2,39] Nonetheless, given the overall negative charge on both the EPS and the carboxylated nAg, little accumulation of the nAg was expected nor observed in the biofilm matrix. Furthermore, the sorption of the nAg by *P. fluorescens* was consistent with recent work that reported an important extracellular accumulation of nAg in the biofilms of *P. aeruginosa*.[40] Silver particles smaller than 10 nm have been shown to be enriched by the bacterial membranes of *E. coli* and *P. aeruginosa*, and particles up to 80 nm have been shown to penetrate the outer membrane.[41,42] Nonetheless, electrostatic arguments alone do not appear to be sufficient to explain the accumulation of the nanoparticles. For *E. coli*, no differences in sorption to the bacterial cells or growth rate were observed when comparing positively and negatively charged nAg.[43]

While it is not surprising that nAg immobilization by the bacteria resulted in a lowering of the overall diffusive flux through the biofilm, it is surprising that the self-diffusion coefficient, as measured by FCS, was decreased to this extent. FCS measures local diffusion of the particles via their fluorescence intensity fluctuations, and thus, if the particles are completely immobile, they should correlate at very long times that do not contribute to the calculation of D. It is, thus, likely that the smaller than predicted diffusion coefficients of nAg that were measured in the dense biofilms reflected the coupled diffusion of nAg and biofilm components, such as the extracellular proteins and the bacteria themselves.

Environmental Implications. Knowledge on nanoparticle diffusivity is necessary in order to understand the mobility, aggregation, and toxicity of these compounds in the natural environment. Mutual diffusion may be hindered by: (i) the porous structure of the biofilm; (ii) the local accumulation of the nanoparticles by cells, nondiffusing macromolecules, or the polysaccharide network, and (iii) the adsorption of the solute to freely diffusing species, abiotic particles, or gas bubbles.[6] Self-diffusion of the uncharged dextrans and microspheres was highly dependent upon the size of the nanoparticles and the porosity of the biofilm. The effective pore size of both of the biofilms was clearly in the nanoparticle size range, strongly suggesting that the mobility of nanoparticles, especially larger ones, will be greatly reduced in natural waters and soils. Indeed, for particles with sizes >50 nm, very little penetration of the biofilm occurred, suggesting that the transport of larger colloids or bacteriophages would be greatly hindered while the diffusion of molecular sized solutes would be only slightly (ca. 30%) affected by the presence of biofilms. Nonetheless, the role of biofilm composition was significant, even for two biofilms produced from the same

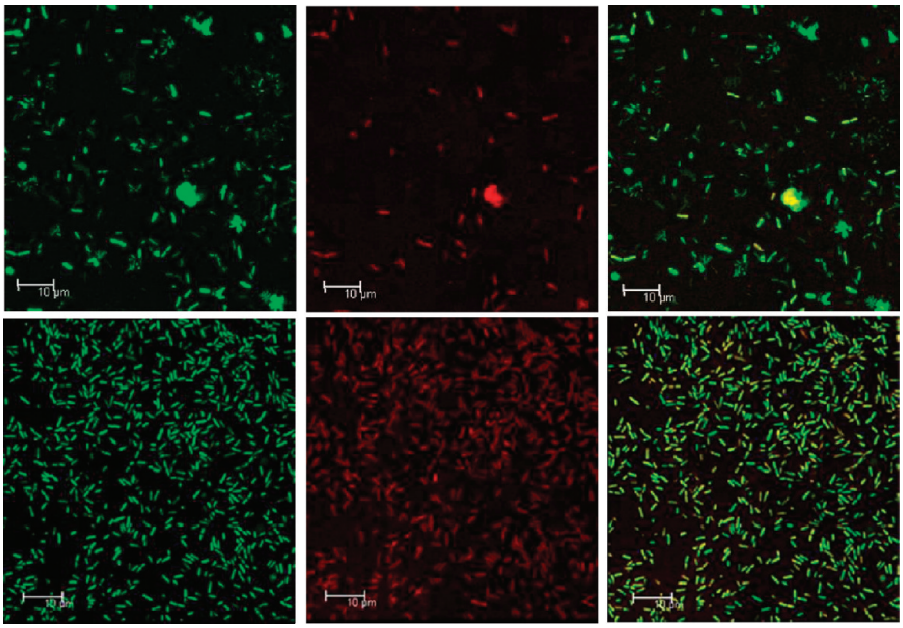

Figure 5. Confocal laser scanning microscopy of *P. fluorescens* microcolonies grown under different total Fe concentrations. Top: 0.1 mM of added Fe(III); bottom: 0.01 mM Fe(III); left: bacterial cells stained with Syto9 to show viable cells; middle: fluorescence of labeled nAg; right: overlay of the Syto9- and nAg-fluorescence. nAg were labeled using Nile Blue A which was excited using a 633 nm HeNe laser while Syto9 was excited with the 488 nm line of an Ar ion laser. The nAg was mainly associated with biofilm components in close proximity to the bacterial cells.

monoculture (ca. 1 order of magnitude difference observed in D_{bio}).

Another important factor was the chemical composition of the nanoparticle. The adsorption and accumulation of nAg by bacteria in the biofilm resulted in a significant reduction in its diffusive flux. In contrast, the substantial increase in the concentration of nAg in the immediate, local environment of the bacteria would likely result in increased bioavailability as compared to the exposure of planktonic organisms. On the basis of the above, the decreased susceptibility of biofilms toward antimicrobial agents, including nAg, may be caused by hindered diffusion, retention in the outer biofilm layers, or reduced metabolic activities of the microorganisms.[44] Future studies will be required to quantify the role of biofilm heterogeneity and nanoparticle chemistry on environmental diffusive fluxes.

■ ASSOCIATED CONTENT

Supporting Information. Free volume theory, interpretation of the FCS autocorrelation function, experimental setup description and figure, table of experimentally determined shape parameter ω_{xy}, figure of visual illustration of effect of the parameters in equation 3 on the autocorrelation, figure of autocorrelation of a Dx10k sample measured in water and in a microbial microcolony with different fits to the experimental data, table of average anomalous diffusion parameter α in the two different kinds of microcolonies, figure of the labeling procedure for the nAg, table of amounts of reactants used for the labeling of silver nanoparticles and silver concentrations following labeling, figure of fluorescence emission spectra of labeled and unlabeled silver nanoparticles at different excitation wavelengths, table of FCS-measurement conditions in biofilms, figure of typical time course of the penetration of labeled nAg into bacterial microcolonies, error estimation, relative quantities, table of standard deviations relative to the measured mean diffusion times $\langle \tau_D \rangle$ for repeated FCS measurements in water and in the microcolonies, histograms of the measured relative diffusion times, table of parameters obtained by fitting Gaussians to histograms of the relative diffusion coefficients, absolute quantities, and table of measured diffusion coefficients in water and corresponding hydrodynamic radii. This material is available free of charge via the Internet at http://pubs.acs.org.

■ AUTHOR INFORMATION

Corresponding Author

*Phone: +1-514 343 6741; fax: +1-514 343 7586; e-mail: kj.wilkinson@umontreal.ca.

Present Addresses

‡Institute of Molecular Physical Chemistry, Heinrich-Heine-University Düsseldorf, Building 26.32.02, Universitätsstrasse 1, 40225 Düsseldorf, Germany.

■ ACKNOWLEDGMENT

The authors gratefully acknowledge the support of NSERC and the FQRNT team research grants program. This project also received some financial support of the Government of Canada through the Department of the Environment. We also appreciate the donation of nAg from Vive Nano and technical assistance from Elena Nadezhina on the biofilm.

■ REFERENCES

(1) Wingender, J., Neu, T. R., Flemming, H. C., Eds. Microbial extracellular polymeric substances—Characterisation, structure and function; Springer: Berlin, 1999.

(2) Jahn, A.; Griebe, T.; Nielsen, P. H. Composition of *Pseudomonas putida* biofilms: Accumulation of protein in the biofilm matrix. *Biofouling* **1999**, *14* (1), 49–57.

(3) Flemming, H. C.; Wingender, J. Relevance of microbial extracellular polymeric substances (EPSs)—Part I: Structural and ecological aspects. *Water Sci. Technol.* **2001**, *43* (6), 1–8.

(4) Leon-Morales, C. F.; Leis, A. P.; Strathmannm; Flemming, H. C. Interactions between laponite and microbial biofilms in porous media: implications for colloid transport and biofilm stability. *Water Res.* **2004**, *38*, 3614–3626.

(5) Strathmann, M.; Leon-Morales, F.; Flemming, H. C. In Influence of biofilms on colloid mobility in the subsurface; Frimmel, F. H.; Kammer, F.; Flemming, H. C., Eds.; Springer: Berlin, 2007; pp 143−173.

(6) Stewart, P. S. Diffusion in biofilms. *J. Bacteriol.* **2003**, *185* (5), 1485–1491.

(7) Stewart, P. S. A review of experimental measurements of effective diffusive permeabilities and effective diffusion coefficients in biofilms. *Biotechnol. Bioeng.* **1998**, *59* (3), 261–272.

(8) Takenaka, S.; Pitts, B.; Trivedi, H. M.; Stewart, P. S. Diffusion of macromolecule in model oral biofilms. *Appl. Environ. Microbiol.* **2009**, *75*, 1750–1753.

(9) Lawrence, J.; Wolfaardt, G. M.; Korber, D. R. Determination of diffusion coefficients in biofilms by confocal laser microscopy. *Appl. Environ. Microbiol.* **1994**, *60* (4), 1166–1173.

(10) Marcotte, L.; Barbeau, J.; Lafleur, M. Characterization of the diffusion of polyethylene glycol in Streptococcus mutans biofilms by Raman microspectroscopy. *Appl. Spectrosc.* **2004**, *58* (11), 1295–1301.

(11) Bryers, J. D.; Drummond, F. Local macromolecule diffusion coefficients in structurally non-uniform bacterial biofilms using fluorescence recovery after photobleaching (FRAP). *Biotechnol. Bioeng.* **1998**, *60* (4), 462–473.

(12) Briandet, R.; Lacroix-Gueu, P.; Renault, M.; Lecart, S.; Meylheuc, T.; Bidnenko, E.; Steenkeste, K.; Bellon-Fontaine, M.-N.; Fontaine-Aupart, M.-P. Fluorescence correlation spectroscopy to study diffusion and rection of bacteriophages inside biofilms. *Appl. Environ. Microbiol.* **2008**, *74* (7), 2135–2143.

(13) Guiot, E.; Georges, P.; Brun, A.; Fontaine-Aupart, M. P.; Bellon-Fontaine, M. N.; Briandet, R. Heterogeneity of diffusion inside microbial biofilms determine by fluorescence correlation spectroscopy under two-photon excitation. *J. Photochem. Photobiol.* **2002**, *75* (6), 570–578.

(14) Lacroix-Gueu, P.; Briandet, R.; Leveque-Fort, S.; Bellon-Fontaine, M. N.; Fontaine-Aupart, M. P. In situ measurements of viral part diffusion inside mucoid biofilms. *C.R. Biol.* **2005**, *328*, 1065–1072.

(15) Zhang, Z.; Wilkinson, K. J. 2011 Quantifying diffusion in a biofilm of *Streptococcus mutans*. *Antimicrob. Agents Chemother.* **2011**, *55*, 1075–1081.

(16) Vogt, M.; Flemming, H. C.; Veeman, W. S. Diffusion in Pseudomonas aeruginosa biofilms: a pulsed field gradient NMR study. *J. Biotechnol.* **2000**, *77* (1), 137–146.

(17) Fatin-Rouge, N.; Buffle, J. In *Environmental Colloids and Particles*; Wilkinson, K. J., Lead, J. R., Eds. IUPAC: Chichester, 2007; pp 508−547.

(18) Rigler, R.; Mets, U.; Widengren, J.; Kask, P. Fluorescence correlation spectroscopy with high cout rate and low background: analysis of translational diffusion. *Eur. Biophys. J.* **1993**, *22*, 169–175.

(19) Magde, D.; Elson, E. L. Fluorescence correlation spectroscopy II: An experimental realization. *Biopolymers* **1974**, *13*, 29–61.

(20) Widengren, J.; Scheinberger, E.; Berger, S.; Seidel, C. A. M. Two new concepts to measure fluorescence resonance energy transfer via fluorescence correlation spectroscopy: Theory and experimental realizations. *J. Phys. Chem. A* **2001**, *105*, 6851–6866.

(21) Enderlein, J.; Gregor, I.; Patra, D.; Dertinger, T.; Kaupp, U. B. Performance of fluorescence correlation spectroscopy for measuring diffusion and concentration. *ChemPhysChem* **2005**, *6*, 2324–2336.

(22) Petersen, N. O.; Elson, E. L. Measurement of diffusion and chemical kinetics by fluorescence photobleaching recovery and fluorescence correlation spectroscopy. *Methods Enzymol.* **1986**, *130*, 454–484.

(23) Moussaoui, M.; Benlyas, M.; Wahl, P. Diffusion of proteins in Sepharose Cl-B gels. *J. Chromatogr.* **1998**, *591* (1−2), 115–120.

(24) Yasuda, H.; Lamaze, C. E.; Ikenberry, L. D. Permeability of solutes through hydrated polymer membranes Part 1: Diffusion of sodium chloride. *Makromol. Chem.* **1968**, *118*, 19–35.

(25) Amsden, B. Solute Diffusion within Hydrogels, Mechanisms and Models. *Macromolecules* **1998**, *31*, 8382–8395.

(26) Compeau, G.; Al-Achi, B. J.; Plastsouka, E.; Levy, S. B. Survival of rifampin-resistant mutants of Pseudomonas fluorescens and Pseudomonas putida in soil system. *Appl. Environ. Microbiol.* **1988**, *54* (10), 2432–2438.

(27) Laguecir, A.; Ulrich, S.; Labille, J.; Fatin-Rouge, N.; Stoll, S.; Buffle, J. Size and pH effect on electrical and conformational behavior of poly(acrylic acid): Simulation and experiment. *Eur. Polym. J.* **2006**, *42* (5), 1135–1144.

(28) Domingos, R. F.; Baalousha, M. A.; Ju-Nam, Y.; Reid, M. M.; Tufenkji, N.; Lead, J. R.; Leppard, G. G.; Wilkinson, K. J. Characterizing manufactured nanoparticles in the environment: Multimethod determination of particle sizes. *Environ. Sci. Technol.* **2009**, *43*, 7277–7284.

(29) Domingos, R. F.; Tufenkji, N.; Wilkinson, K. J. Aggregation of titanium dioxide nanoparticles: Role of a fluvic acid. *Environ. Sci. Technol.* **2009**, *43* (5), 1282–1286.

(30) Gendron, P. O.; Avaltroni, F.; Wilkinson, K. J. Diffusion coefficients of several rhodamine derivatives as determined by pulsed field gradient-nuclear magnetic resonance and fluorescence correlation spectroscopy. *J. Fluoresc.* **2008**, *18* (6), 1093–1101.

(31) Müller, C. B.; Loman, A.; Pacheco, V.; Koberling, F.; Willbold, D.; Richtering, W.; Enderlein, J. Precise measurement of diffusion by multi-color dual-focus fluorescence correlation spectroscopy. *Europhys. Lett.* **2008**, *83*, 46001–46006.

(32) Ioan, C. E.; Aberle, T.; Burchard, W. Structure properties of Dextrans. 2. Dilute solution. *Macromolecules* **2000**, *33* (15), 5730–5739.

(33) Armstrong, J. K.; Wenby, R. B.; Meiselman, H. J.; Fisher, T. C. The hydrodynamic radii of macromolecules and their effect on red blood cell aggregation. *Biophys. J.* **2004**, *87*, 4259–4270.

(34) O'Toole, G. A.; Kolter, R. Initiation of biofilm formation in *Pseudomonas fluorescens* WCS365 proceeds via multiple, convergent signalling pathways: A genetic analysis. *Mol. Microbiol.* **1998**, *28* (3), 449–461.

(35) Buffle, J.; Wilkinson, K. J.; van Leeuwen, H. P. Chemodynamics and Bioavailability in Natural Waters. *Environ. Sci. Technol.* **2009**, *43*, 7170–7174.

(36) Elliot, R. P. Some properties of pyoverdine, the water-soluble pigment pf Pseudomonas. *Appl. Microbiol.* **1958**, *6*, 241–246.

(37) Sanabria, H.; Kubota, Y.; Waxham, M. N. Multiple diffusion mechanisms due to nanostructuring in crowded environments. *Biophys. J.* **2007**, *92* (1), 313–322.

(38) Fatin-Rouge, N.; Starchev, K.; Buffle, J. Size effects on diffusion processes within agarose gels. *Biophys. J.* **2004**, *86*, 271–2719.

(39) Palmgren, R.; Nielsen, P. H. Accumulation of DNA in the exopolymeric matrix of activated sludge and bacterial cultures. *Water Sci. Technol.* **1996**, *34* (5−6), 233–240.

(40) Fabrega, J.; Renshaw, J. C.; Lead, J. R. Interactions of silver nanoparticles with *Pseudomonas putida* biofilms. *Environ. Sci. Technol.* **2009**, *43*, 9004–9009.

(41) Morones, J. R.; Elechiguerra, J. L.; Camacho, A.; Holt, K.; Kouri, J. B.; Ramirez, J. T.; Yacaman, M. J. The bactericidal effect of silver nanoparticles. *Nanotechnology* **2005**, *16*, 2346–2353.

(42) Xu, X. H. N.; Brownlow, W. J.; Kryriacou, S. V.; Wan, Q.; Viola, J. J. Real-time probing of membrane transport in living microbial cells using single nanoparticle optics and living cell imaging. *Biochemistry* **2004**, *43*, 10400–10413.

(43) Dror-Ehre, A.; Mamane, H.; Belekova, T.; Markovich, G.; Adin, A. Silver nanoparticle−*E. coli* colloidal interaction in water and effect on *E. coli* survival. *J. Colloid Interface Sci.* **2009**, *339* (2), 521–526.

(44) Costerton, J. W.; Stewart, P. S.; Greenberg, E. P. Bacterial biofilms: a common cause of persistent infections. *Science* **1999**, *284*, 1318–1322.